AI-Based Landmark Detection for Condylar Asymmetry Assessment in Patients with Juvenile Idiopathic Arthritis

Michele Signori[1], Mattia Savardi[2], Martina Cattadori[2,3], Ingrid Tonni[2,3], Alberto Signoroni[2]

[1] Department of Information Engineering, Università di Brescia, Italy
[2] Department of Medical and Surgical Specialties, Radiological Sciences, and Public Health, Università di Brescia, Italy
[3] Dental School, Università di Brescia, Italy

Repository

Introduction

- **Motivation:** JIA can affect the temporomandibular joint (TMJ), leading to **condylar alterations** and facial deformities, therefore **early diagnosis** is crucial to limit disease-related damage.
- **Solution:** Evaluation of **condylar asymmetry** through the **automatic identification** of anatomical landmarks in OPG images, which are widely used as **first-line** modality because of their **lower radiation exposure**.
- **Main contributions**:
  - **Deep learning** model for **automatic landmark annotation** on both healthy and JIA-affected patients.
  - Evaluation of **condylar asymmetry indices** via their ability to discriminate between JIA and healthy cohorts.
  - **Web-based annotation tool** to streamline landmark labelling workflow for dental clinicians.

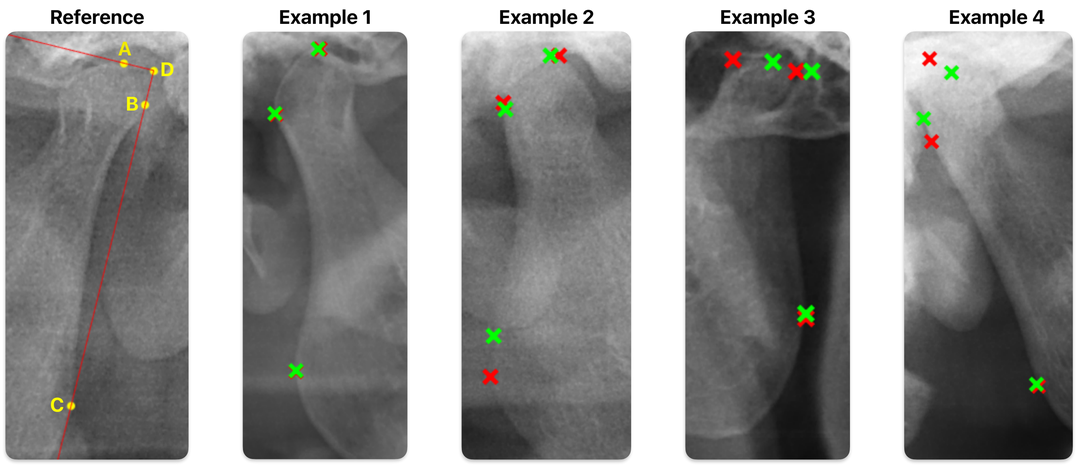

Reference image showing landmark positions and examples of annotations by two experts on 4 pathological cases

Dataset and Annotation Tool

- **Dataset**: **188** annotated **OPG images** of patients between 10 and 30 years old. Of these, **125** images belong to patients **without JIA**, while the remaining **63** belong to patients diagnosed **with JIA**.
- **Manual Landmark Annotation Tool:** Developed to accelerate and standardize OPG upload, anonymization, and the annotation of specific landmarks required to compute the Habets index[1].

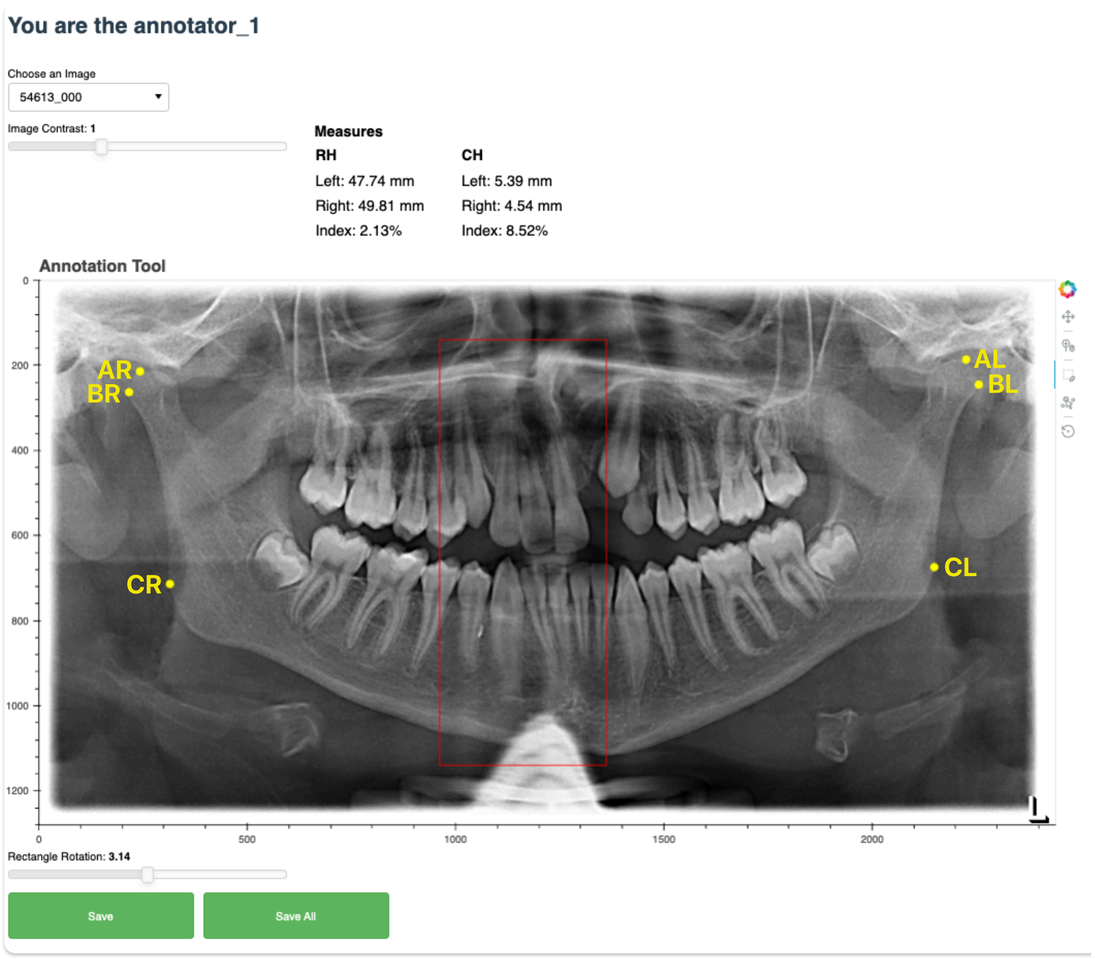

[1] Habets, L. L. M. H., et al. "The Orthopantomogram®, an aid in diagnosis of temporomandibular joint problems. II. The vertical symmetry." *Journal of oral rehabilitation* 15.5 (1988): 465-471.

Methods

- **Asymmetry Index Evaluation:** Exploratory analysis of the discrimination performance of **55** different **asymmetry indexes** derived from the six annotated landmarks.
- **Automatic Landmark Annotation Model:** Adapted implementation of the **Spatial Configuration Network** (SCN)[2].
  - **Two components**: **local appearance** that focuses on **locally accurate** but ambiguous candidates, and **spatial configuration**, to **improve robustness** towards landmark misidentification by reducing ambiguities.

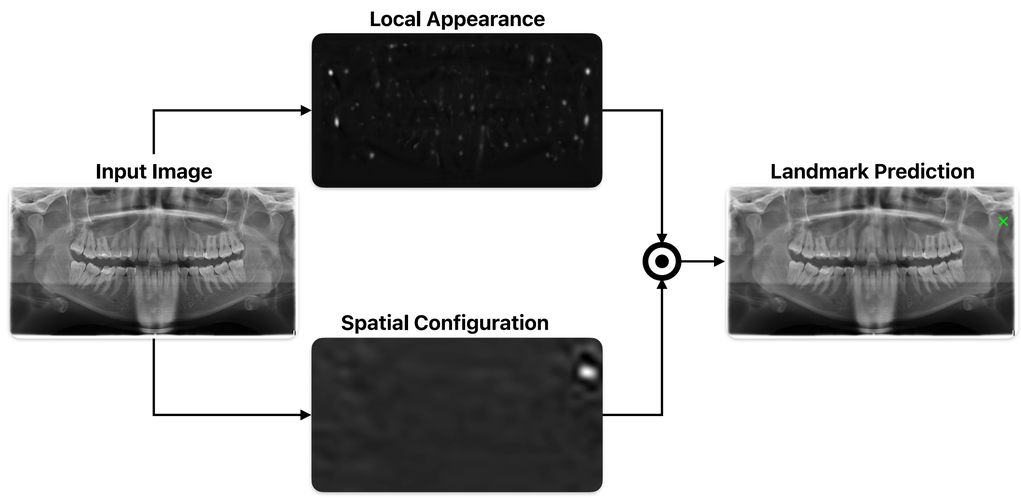

Example of the prediction of the landmark B with the SCN pipeline

[2] Payer, Christian, et al. "Integrating spatial configuration into heatmap regression based CNNs for landmark localization." Medical image analysis 54 (2019): 207-219.

Results

Localization accuracy of automatic landmark detection model on full dataset and separately for normal and pathological images. We report both MAE and SDR @ 2,3,4 mm for single landmarks and globally.

Landmark	Full Dataset				Normal				Pathological			
	MRE ± SD (mm)	SDR (%)			MRE ± SD (mm)	SDR (%)			MRE ± SD (mm)	SDR (%)		
		2 mm	3 mm	4 mm		2 mm	3 mm	4 mm		2 mm	3 mm	4 mm
AL	1.52 ± 2.60	79.79	92.55	96.81	1.34 ± 0.97	80.00	92.00	98.40	1.88 ± 4.25	79.37	93.65	93.65
BL	1.26 ± 1.93	82.98	92.02	96.28	1.21 ± 1.16	81.60	92.80	96.00	1.38 ± 2.90	85.71	90.48	96.83
CL	1.98 ± 2.51	69.15	83.51	88.83	2.18 ± 2.70	64.80	81.60	87.20	1.58 ± 2.02	77.78	87.30	92.06
AR	1.68 ± 2.33	77.13	86.17	94.68	1.44 ± 1.36	80.80	87.20	96.00	2.16 ± 3.50	69.84	84.13	92.06
BR	1.13 ± 1.76	89.36	94.68	97.87	1.05 ± 0.97	88.00	93.60	97.60	1.28 ± 2.72	92.06	96.83	98.41
CR	1.89 ± 2.45	70.74	84.04	89.89	1.96 ± 2.36	68.80	84.00	88.80	1.77 ± 2.61	74.60	84.13	92.06
Global	1.58 ± 2.31	78.19	88.83	94.06	1.53 ± 1.78	77.33	88.53	94.00	1.68 ± 3.10	79.89	89.42	94.18

Agreement between **manual annotators** and between **model predictions and GT** for the main measures, i.e. Condylar Height and Ramal Height.

Measure	Annotators		Pred. vs. GT	
	MAE ± SD (mm)	ICC [95% CI]	MAE ± SD (mm)	ICC [95% CI]
CH (left)	0.85 ± 0.81	0.870 [0.79, 0.91]	1.18 ± 1.23	0.716 [0.64, 0.78]
CH (right)	0.86 ± 0.88	0.849 [0.80, 0.89]	1.07 ± 0.92	0.778 [0.72, 0.83]
RH (left)	1.47 ± 1.41	0.928 [0.88, 0.95]	1.96 ± 2.44	0.813 [0.76, 0.86]
RH (right)	1.54 ± 1.33	0.931 [0.91, 0.95]	1.88 ± 1.88	0.866 [0.82, 0.90]

Top-ranked asymmetry indexes by AUC for normal vs JIA classification, together with MAE, Precision and Recall. Bold values highlight **standard CH index** and **ABC angle** as potential CH alternative.

Index	MAE (%)	AUC [95% CI]	Precision	Recall
$\overline{BD}/\angle BAC$	14.530	0.688 [0.598, 0.775]	0.544	0.587
$\overline{\mathbf{BD}}$**(CH)**	**8.380**	**0.683 [0.595, 0.760]**	**0.532**	**0.524**
$\overline{AB}/\angle BAC$	11.830	0.672 [0.582, 0.752]	0.493	0.556
$\overline{AB}/\overline{BD}$	5.800	0.670 [0.586, 0.750]	0.526	0.476
$(\overline{BD}+\overline{CD})/\angle BAC$	9.910	0.664 [0.582, 0.750]	0.487	0.603
$\overline{BD}/\angle BCA$	12.200	0.660 [0.579, 0.746]	0.466	0.540
$\angle$**ABC**	**2.380**	**0.660 [0.576, 0.742]**	**0.458**	**0.524**
$\overline{AD}/\overline{BD}$	11.510	0.658 [0.576, 0.740]	0.473	0.556
$\overline{AC}/\angle BAC$	9.320	0.657 [0.573, 0.743]	0.467	0.556
$\overline{CD}/\angle BAC$	9.360	0.656 [0.575, 0.741]	0.467	0.556

Conclusion

- **Validation** of automated landmark localization across varying degrees of pathological condylar morphology.
- **Confirmation** of the clinical relevance of condylar measures (e.g., Habets CH index), highlighting the necessary trade-off between discriminative capability and robustness to model-predicted variance.
- **Future development** of a human-in-the-loop workflow to accelerate clinical annotation via AI-initialized landmark suggestions.